

Critical slowing down in polymer dynamics near the coil-stretch transition in elongation flow

Sergiy Gerashchenko and Victor Steinberg

Department of Physics of Complex Systems, Weizmann Institute of Science, Rehovot, 76100 Israel

(Received 7 May 2007; revised manuscript received 28 August 2008; published 14 October 2008)

We present experimental results on relaxation dynamics of λ -DNA and T4 polymer molecules toward a steady state in elongation flow. Strong critical slowing down (similar to the well-known effect in continuous phase transitions) in polymer relaxation near the coil-stretch transition (CST) is quantitatively investigated and found to be in good accord with predictions. For polymers with a small number of Kuhn segments the maximum of the relaxation time vs the strain rate provides precise information about the location of the CST and serves as its criterion.

DOI: [10.1103/PhysRevE.78.040801](https://doi.org/10.1103/PhysRevE.78.040801)

PACS number(s): 83.80.Rs, 47.57.Ng

During the last decade impressive progress in our understanding of the dynamics and conformation of an individual polymer molecule in an elongation flow became possible due to the development of single-molecule visualization via fluorescence microscopy [1,2]. Quantitative characterization of the velocity field and DNA molecule stretching dynamics and statistics as well as the use of extremely low polymer concentrations to avoid polymer interaction and feedback effect on the flow allowed accurate comparison with numerical simulations. In regard to the experimental results reported in this Rapid Communication, we single out two central observations in the dynamics of a DNA molecule in an elongation flow, namely, the experimental verification of the theoretically predicted existence of a sharp coil-stretch transition (CST) in molecular conformation [1], and conformational hysteresis at the CST for extremely long DNA molecules ($L \approx 1.3$ mm, which is equivalent to about $N=10\,000$ Kuhn segments, where L is the polymer contour length) [3]. Both results have had a profound impact on the development of constitutive models for polymer solutions that provide the basis for a hydrodynamic description of polymer solution flows. It has been realized that the CST in polymer conformation has a direct influence on the flow dynamics of a polymer solution at large scales, and thus is essential for solving the turbulent drag reduction problem [4].

Recently, theory and numerical simulations of a dynamical slowdown in a single-polymer relaxation near the CST were reported [5,6]. It was shown that in the elongation flow near the CST the polymer relaxation time to a steady-state configuration determined as an ensemble-averaged time T became much longer than the Zimm relaxation time [7] and had a peak value at the transition point. This effect is a characteristic feature and unique signature of the CST and one of the striking manifestations of a dramatic influence of the flow on single-polymer dynamics. The main physical reason for the strong increase of the polymer relaxation time is the large number of polymer configurations corresponding to vastly different end-to-end distances that are available close to the CST, where the entropic, elastic force of a molecule is balanced by the hydrodynamic drag force exerted on the molecule by the elongation flow [5,6]. Moreover, the slowdown is dramatically enhanced by the conformation-dependent drag force [6], an effect that is closely related to the conformational hysteresis predicted by de Gennes a long time ago [8] and confirmed experimentally just recently [3].

Thus, two distinguishing features of the CST, the slowdown of polymer dynamics and the hysteresis in polymer conformations, can be used as a criterion for an experimental determination of the CST. The peak value T_{\max} in the polymer relaxation time dependence on the strain rate $\dot{\epsilon}$ in the vicinity of the CST allows precise location of the transition point [5,6], particularly for polymer molecules with a relatively small number of Kuhn segments, where the conformational hysteresis is unobservable. The definition of a CST as a “sharp and steep” change between coil and extended polymer configurations, used for its characterization in Ref. [1], indicates a qualitative approach to the problem, while the slowdown in the polymer relaxation suggests a quantitative criterion. Furthermore, even in the recent experiment [3], the conformational hysteresis resulting from the conformation-dependent drag was observed only for the longest DNA molecules with a two orders of magnitude larger number of Kuhn segments than in λ -DNA. According to recent numerical simulations [9], the hysteresis is expected to be observed for molecules with drag ratio above 4.5, about the same value that was found for the molecule first showing the hysteresis [3].

The functional shape of the relaxation time T versus $\dot{\epsilon}$ also helps to straighten out the controversial problem of a suggested similarity of the coil-stretch and a first-order transition, which was first discussed in the infinite molecular weight limit in Ref. [8] and further described in Ref. [3]. Based just on the observations of the hysteresis and its disappearance for lower molecular weight polymers, the authors of Ref. [3] made a far-reaching conclusion that the transition bears a full analogy with a first-order thermodynamical phase transition, where the strain rate plays the role of pressure, the steady-state fractional extension that of molar volume, and the inverse molecular weight M^{-1} that of temperature. Then the possible existence of the critical point of the CST at some M_c^{-1} , above which a continuous gradual transition between the coil and stretch states should be observed [3], was postulated.

However, the theoretically suggested functional form of the polymer relaxation time versus $\dot{\epsilon}$ [5,6], which persists for values of the drag ratio up to 8, corresponding to extremely long molecules, is very different from that known from the dynamics of the first-order phase transition [10]. Indeed, for the first-order transition the inverse transition rate decreases

TABLE I. Geometrical parameters (R_g is the gyration radius, d is the molecule diameter), the polymer longest relaxation time τ_{rel} , number of Kuhn elements N , and drag ratio ζ_r/ζ_c for λ -DNA and T4 molecules, and corresponding solvent viscosities η are presented.

Molecule	L (μm)	R_g (μm)	d (μm)	η (Pa s)	τ_{rel} (s)	N	ζ_r/ζ_c
λ	21 ± 1	0.73	0.002	0.02	2.02(0.04)	150	1.6
T4	67 ± 2	1.64	0.002	0.00275	2.15(0.1)	525	2.1

due to increased probability of nucleation of a stable phase from infinity at the coexistence curve to zero at the spinodal. These considerations show that an experimental verification of the slowdown effect in the polymer relaxation dynamics would be critically important to resolve the issues discussed above.

The experiments were conducted at the stagnation point of symmetric cross-slot micro channel geometry. The micro-channel of $650 \mu\text{m}$ wide and $150 \mu\text{m}$ in height was manufactured in elastomer (polydimethylsiloxane) by soft lithography [11]. The experimental setup was temperature controlled within 22 ± 0.05 °C. To minimize flow rate fluctuations, a gas-tight $100 \mu\text{l}$ syringe driven via a micrometer head by an encoder feedback-controlled dc motor with 1.0% rms fluctuations was used. The location of the stagnation point was tuned hydrostatically by varying the relative height of the two channel outlets with a computer-controlled stepping motor. Another fine adjustment within $\pm 8 \mu\text{m}$ of the location of the objective focal plane with respect to the microchannel by a computer-controlled stepping motor was available in the case when a molecule deviated from the focal plane due to Brownian motion.

To study the dynamics and statistics of polymer stretching in an elongation flow we used two types of molecules, λ -DNA and T4, in concentration 10^{-3} ppm, fluorescently stained with YOYO-1 (Molecular Probes) at a dye:base ratio of 1:4 for ~ 1 h. As the working fluid a buffer solvent [12] was prepared with two concentrations of sucrose to tune the polymer Zimm relaxation time τ_{rel} for both DNA molecules into the same range. The Zimm relaxation times of both λ -DNA and T4 molecules averaged on about 60 molecules were measured and analyzed as in Refs. [1,13]. All relevant parameters characterizing both λ -DNA and T4 are presented in Table I.

Fluorescently labeled DNA molecules were monitored via a $63\times$, numerical aperture 1.4, oil immersion objective (Zeiss) with $0.4 \mu\text{m}$ focus depth and $\sim 190\text{-}\mu\text{m}$ -long working distance with a homemade epifluorescent microscope [13]. Single DNA molecules were imaged at the half-height of the microchannel by an intensified charge-coupled device video camera (Video Scope 350F), and the digitized images were transferred through a frame grabber directly to a computer with the frame speed of 12.5 frames/s. To reduce photobleaching, single molecules were illuminated stroboscopically at about 40 Hz (i.e., $\epsilon\Delta t < 0.2$) using a mechanical shutter synchronized with the camera. So the total illumination time during an experiment was about 11 s for λ -DNA and 20 s for T4. To avoid any predeformation, the molecule was first trapped at the stagnation point by using feedback control and was kept at zero flow for $\sim 8\tau_{\text{rel}}$ to allow relax-

ation to an initial random coiled state, before the flow was turned on.

The imaging area around the stagnation point ($90 \times 90 \mu\text{m}$) was used as the flow calibration region. Flow velocity profiles in both the vertical and horizontal planes were measured by particle tracking velocimetry (PTV) using $1 \mu\text{m}$ fluorescent beads, and compared well with the numerical simulations. In the vertical plane the shear rate varied within $\pm 8 \mu\text{m}$ deviation from the center up to 2%, while in the horizontal plane $\dot{\epsilon}$ changed not more than 2% across the imaging region and depended linearly on the motor speed.

Measurements of the averaged fractional extensions $\langle R \rangle/L$ of λ -DNA molecules as a function of either the residency time t or the accumulated strain $\dot{\epsilon}t$ for 11 different values of the Weissenberg number $Wi = \dot{\epsilon}\tau_{\text{rel}}$ in the vicinity of the CST at $Wi_c \approx 0.5$ [8] are presented in Fig. 1 (six values are shown). Similar data were collected for T4-DNA for eight values of Wi . Measurements of individual traces on up to 270 molecules for each value of Wi were used. In the most sensitive region near the CST the following numbers of molecules were used for analysis: for λ -DNA 204 at $Wi=0.38$, 55 at $Wi=0.4$, 271 at $Wi=0.43$, 107 at $Wi=0.48$, and 110 at $Wi=0.52$; for T4 55 at $Wi=0.34$, 136 at $Wi=0.42$, 64 at $Wi=0.49$, 118 at $Wi=0.52$, and 83 at $Wi=0.55$ [14]. The data were taken for a relatively long residency time (up to $\dot{\epsilon}t \approx 30$) to ensure the saturation of the average extension in the steady state for both DNA molecules (Figs. 2 and 3). From the data in Figs. 1–3, one can notice two main features of the molecular stretching dynamics. The closer the value of Wi to the critical one, Wi_c , the wider the molecule extension distribution and the longer the residency time to reach the steady state. These features are similar to those exhibited by

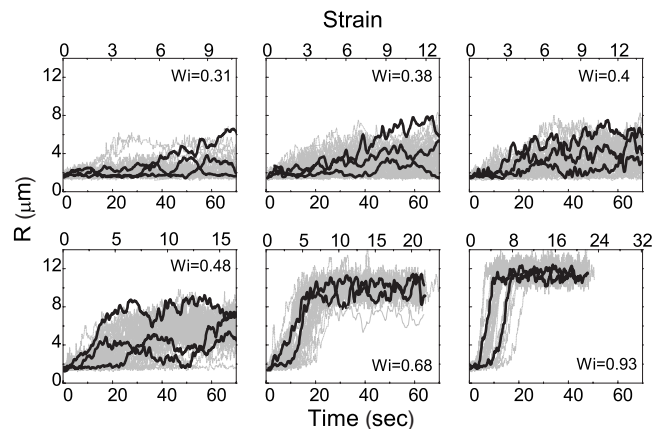


FIG. 1. Extensions of individual λ -DNA molecules versus either residency time t or strain $\dot{\epsilon}t$, for six values of Wi . Several individual traces are highlighted.

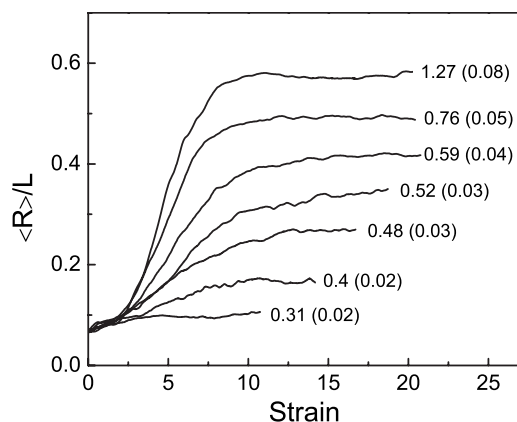


FIG. 2. Average fractional extension $\langle R \rangle/L$ of λ -DNA molecules versus strain for seven values of Wi .

a macroscopic system due to the balance between energy and entropy in the vicinity of a continuous (second-order) thermodynamic phase transition. The balance leads to a flat minimum in a thermodynamic potential and a large number of available states, and results in large thermodynamic fluctuations and the critical slowing down (see, e.g., [10]). Indeed, the inset in Fig. 5 illustrates the dependence of the reduced molecule extension fluctuations in the steady state, $\Delta R/L$, as a function of Wi for both DNA molecules, with a particularly pronounced peak at $Wi_c \approx 0.5$ for T4 molecules, where $\Delta R = \sqrt{\langle (R - \langle R \rangle)^2 \rangle}$. These intrinsic features of the CST as well as of the second-order transition drastically complicate the experiment and limit the possibility of reaching a steady state. Near the CST t_{res} of the observation of a single molecule is limited due to the photobleaching. Thus, experimental limitations due to photobleaching as well as enhanced molecule extension fluctuations near the CST considerably hamper reaching the steady state near the CST. It became obvious particularly for longer T4 molecules at values of $Wi = 0.42, 0.49, 0.52$ (see Fig. 3).

Figure 4 presents a comparison of the maximum steady-state extensions R_{max} reached at each Wi found in the current experiment for both DNA molecules compared with those obtained in Ref. [1]. Rather close agreement between the

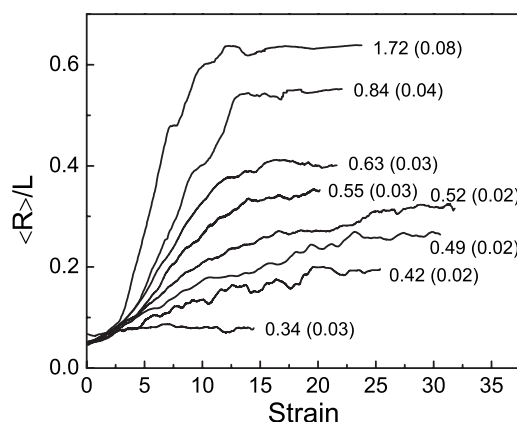


FIG. 3. Average fractional extension $\langle R \rangle/L$ of T4 molecules versus strain for eight values of Wi .

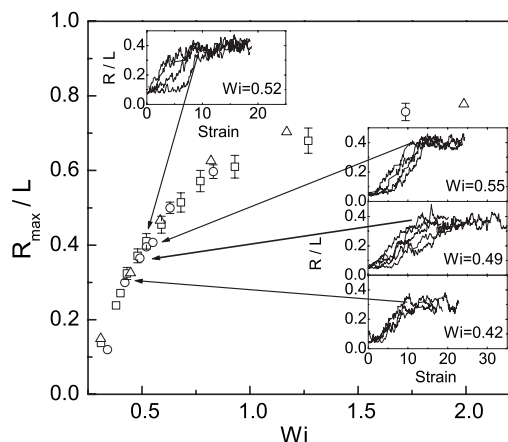


FIG. 4. Maximum steady-state extension, R_{max}/L , versus Wi for λ -DNA (squares) and T4 (circles) molecules, and λ -DNA (triangles) from Ref. [1]. Several traces of individual molecules with maximum extensions for different Wi are presented in insets.

different data sets is observed. The individual traces that reach the steady state with maximum molecule extensions for different Wi close to Wi_c are presented in the insets in Fig. 4. The individual traces also demonstrate that, in spite of the fact that saturation is not clearly achieved for $\langle R \rangle/L$ in Fig. 2 for $Wi = 0.52$ and in Fig. 3 for $Wi = 0.42, 0.49, 0.52$, and 0.55 , the steady state is definitely reached for the molecules in the insets in Fig. 4.

The relaxation time T as a function of Wi was defined from the following fit of the data presented in Figs. 2 and 3: $\langle RR \rangle = a \tanh(t/T) + c$. The results of this analysis for T/τ_{rel} are presented in Fig. 5 for both λ -DNA and T4. First, maxima T_{max}/τ_{rel} on both curves are clearly observed, and their values for the two molecules differ significantly. Second, the maxima of the two curves are shifted slightly relative to each other, though probably within our resolution in detecting T_{max} . No hysteresis in the peaks' locations was found. One should point out that the ratio between the residency and relaxation times, t_{res}/T , was between 1.8 and 7 for λ -DNA, and between 1.3 and 5 for T4. The lower values of

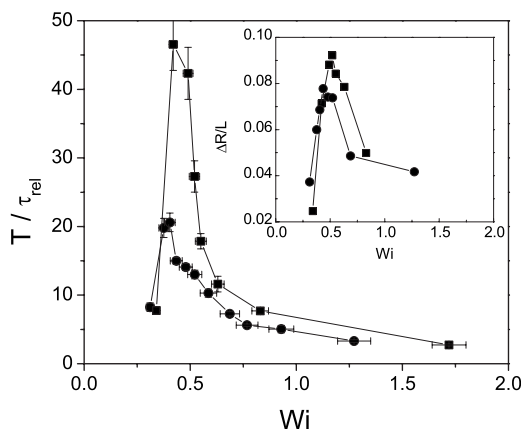


FIG. 5. Scaled relaxation time T/τ_{rel} versus Wi for λ -DNA (dots) and T4 (squares) molecules. Inset: The fractional extension fluctuations at a steady state $\Delta R/L$ versus Wi for the same molecules.

t_{res}/T were found near the CST, since τ_{rel} grows there significantly while t_{res} is limited by photobleaching. From this comparison we conclude that the steady state was reached in our measurements up to the CST. As followed from the theory and numerical simulations [6], two factors are responsible for the value of $T_{\text{max}}/\tau_{\text{rel}}$: $b=(L/R_0)^2$ and ζ_r/ζ_c , where $R_0=\sqrt{6}R_g$ is the mean extension at thermal equilibrium. The first parameter b determines the degree of polymer finite extensibility [7]. The larger b , is the closer the polymer is to an infinitely long linear dumbbell molecule. For such polymer molecules the relaxation time to a steady state in an elongation flow near the CST diverges as $T/\tau_{\text{rel}}\sim 1/|\text{Wi}_c-\text{Wi}|$, where $\text{Wi}_c=0.5$ [5,6]. This divergence is the characteristic feature of a continuous phase transition in an infinite thermodynamic system and is known as critical slowing down [10]. The finite-size effect results in a cutoff of a real singularity leading to a finite value of T_{max} . A second parameter ζ_r/ζ_c defines the hydrodynamic drag ratio for the completely stretched (rod), $\zeta_r=2\pi L\eta/\ln(L/d)$, and the coil, $\zeta_c=9\pi^{3/2}R_g\eta/4$, conformations [15]. Numerical simulations show the role of the interplay between the two parameters in the functional shape of T/τ_{rel} versus Wi and in the peak value $T_{\text{max}}/\tau_{\text{rel}}$ [6]. Rather good agreement between the values of $T_{\text{max}}/\tau_{\text{rel}}$ obtained in the experiment, 20 and ~ 45 (see Fig. 5), and from the numerical simulations, 15 and 35, for λ -DNA and T4, respectively, for the values of these two parameters presented in Table I, is found. Thus, based on the

experiment and the numerical calculations, one can conclude that the longer the molecule contour length (at the same molecule diameter), the sharper the dependence of the relaxation time on Wi and the higher its peak value at the CST.

To summarize, we verified experimentally the predicted slowdown in the relaxation dynamics of ensembles of λ -DNA and T4 polymers toward the steady state near the CST in the elongation flow. We argue that the observed slowing down and enhanced fluctuations are critical effects that occur due to the presence of a large number of possible polymer configurations corresponding to vastly different end-to-end distances near the CST and that are similar to the critical effects in the vicinity of a continuous thermodynamic phase transition. Two factors contribute to the sharpness of the transition and the peak value of the polymer relaxation time at Wi_c : the degree of polymer finite extensibility b and the drag ratio for the two limiting polymer conformations, ζ_r/ζ_c . The larger of both factors are the longer the polymer relaxation time is to the steady state.

We thank A. Celani, D. Vincenzi, and A. Puliafito for numerous discussions and exchange of results of numerical calculations and E. Segre for help with software. This work was supported by grants from the Minerva Foundation, Israel Science Foundation, Israeli Ministry of Science, Culture and Sport, and the Minerva Center for Nonlinear Physics of Complex Systems.

-
- [1] T. Perkins, D. Smith, and S. Chu, *Science* **276**, 2016 (1997); D. Smith and S. Chu, *ibid.* **281**, 1335 (1998).
- [2] T. Perkins, D. Smith, and S. Chu, in *Flexible Chain Dynamics in Elongational Flow*, edited by H. Kausch and T. Nguyen (Springer-Verlag, Berlin, 1999), p. 283.
- [3] Ch. Schroeder, H. Babcock, E. Shaqfeh, and S. Chu, *Science* **301**, 1515 (2003).
- [4] J. Davoudi and J. Schumacher, *Phys. Fluids* **18**, 025103 (2006).
- [5] D. Vincenzi and E. Bodenschatz, *J. Phys. A* **39**, 10691 (2006).
- [6] A. Celani, A. Puliafito, and D. Vincenzi, *Phys. Rev. Lett.* **97**, 118301 (2006).
- [7] R. B. Bird, C. F. Curtiss, R. C. Armstrong, and O. Hassager, *Dynamics of Polymeric Liquids* (Wiley, New York, 1987).
- [8] P. G. de Gennes, *J. Chem. Phys.* **60**, 5030 (1974).
- [9] C.-C. Hsieh and R. Larson, *J. Rheol.* **49**, 1081 (2005).
- [10] L. D. Landau and E. M. Lifschitz, *Statistical Physics* (Pergamon, Oxford, 1980).
- [11] Y. Xia and G. M. Whitesides, *Angew. Chem., Int. Ed.* **37**, 550 (1998).
- [12] A pH 8 buffer consisting of 10 mM tris-HCl, 2 mM ethylene diamine tetra-acetic acid, 10 mM NaCl, 4% β -mercaptoethanol, glucose oxidase ($\sim 50 \mu\text{g/ml}$), and catalase ($\sim 10 \mu\text{g/ml}$), with 62% (w/w) sucrose was used (see, e.g., Ref. [1]).
- [13] S. Gerashchenko, C. Chevillard, and V. Steinberg, *Europhys. Lett.* **71**, 221 (2005).
- [14] We notice that use of more than about 50 molecules changes the relaxation time T to just inside the error bars.
- [15] L. D. Landau and E. M. Lifschitz, *Fluid Mechanics* (Pergamon, Oxford, 1987).